We thank both Martin Lüthi and Victor Tsai for their helpful comments, which have helped greatly improve our manuscript. Our responses to each of their points (in bold) are included below (in italics).

Reply to Martin Lüthi

One point that needs attention is the intermingling of viscous and elastic stresses in the theoretical investigation (section 3). Elastic bending stresses are taken from beam theory, and then suddenly interpreted as viscous stresses. From the discussion it is not clear whether this is done because of the assumption of a Maxwell body, but then one would have to argue why elastic displacements are ignored.

In section 3 we take bending stresses from elastic beam theory and use them in a Maxwell rheological model. With a Maxwell rheology, the stresses in the elastic and viscous components are equal and so this is a reasonable approach. Next, we throw away the elastic deformational component and we justify this for two reasons. Firstly, as we show in appendix A, the time derivative of the across flow shear stress is negligible, and so this elastic term will become very small. Secondly, we are primarily interested in how an ice shelf can generate a nonlinear Msf response to a tidal forcing and this elastic term will only directly yield a linear response. These points are made in the text but could be clearer and so we have emphasised them in the revised manuscript.

It would be helpful to extend several figures, especially Figure 5 (adding τE) and Figure 6 (adding τE, extending it to all three experiments). Additionally, a figure showing time series of forcing, horizontal displacement, velocity, τ_E and strain heating in the shear zone would be most helpful.

Figure 6 is a periodogram and it is unclear how tE could be incorporated, but we agree that a figure showing the time series of forcing etc. would be very useful and this has been added.

One of the strong points of the paper is that no state change in the ice is required to produce the period doubling. However, there are three obvious mechanisms which should be discussed: grain size, fractural weakening and strain heating. All of these effects have been invoked to explain ice stream shear margins, so there is ample pertinent literature.
It seems very likely that these processes are also active in a shelf shear margin, which is very similar to a fatigue experiment in material science. Certainly grain size will adapt to the continuous forcing, the material might suffer damaging, and strain heating (which is a model output) will warm and therefor soften the ice.

We agree that a discussion on these other shear margin processes will greatly add to our paper and we have added one to the discussions.

As a side-note, the authors seem to adopt (as in the recent glaciological literature) the term "full-Stokes" to mean Finite Element model, even if they don't solve the Stokes equation, but a visco-elastic extension thereof. There is no such thing as a "full-Stokes" equation, but "reduced-Stokes" solvers which ignore some terms of the Stokes equation.
This is mentioned in many comments below, but should be consistently purged.

In our numerical treatment we include all terms of the momentum equations, apart from the acceleration terms. In the glaciological literature the resulting form of the momentum equations is commonly referred to as the 'full Stokes' equations, and to remain consistent

with previous work we use this terminology (it is certainly not intended as a substitute for Finite Element model). It is important that a reader understands that our model includes all the equilibrium stress balance terms, as against other commonly used approximations in glaciology such as the SSA/SIA. The term 'reduced-Stokes' is likely to cause confusion in this regard, but we are happy to go with the editor's recommendation and change our terminology accordingly.

Specific comments

29 awkward end of sentence.

Changed the wording.

39 GL has not been defined (meaning grounding line).

Added a definition slightly before this point at the first instance of grounding line in the introduction

40 I think this should be "independent"

Fixed

62 To my understanding the effect should be greatest during periods of highest flexuring rates, i.e. during rising and falling tides. The reason is that viscous stresses are created by viscous deformation.

The reviewer is correct that simply saying the effect is greatest at high and low tide is an oversimplification, however since ice is viscoelastic at tidal frequencies the greatest softening effect will be somewhere between the time of maximum flexural rate and high tide.
For an oscillatory stress (i.e. tidal pressure) acting on a Maxwell material, strain will oscillate at the same frequency but with a phase lag. For an ideal elastic material the lag would be zero, whereas for a viscous material the phase lag would be pi/2. Thus, maximum strain will lag slightly after high and low tide, and so strain rate (i.e. velocity) will be greatest slightly before high and low tide. This can be seen in our new figure and we have reworded the relevant sections to make this point clear.

65 Consequently, also here should be "rising" and "falling" tide (not high and low).

See response above.

69 here again the displacement is alluded to, but that is something elasticity is concerned about.

The point being made here is that during neap tide (when vertical displacements are very small) the effect on ice shelf flow will be negligible. This is fundamental to the mechanism of the paper, since that is what leads to a fortnightly Msf signal in ice shelf displacements.

73 "equally as fast": check the usage of English

Changed to: "at least as fast"

93 "Cauchy" upper case (it's a name)

Fixed

98 There is no "Stokes flow" in these equations, that's just the force balance. (For Stokes flow you need the rheology).

Changed to "force balance"

123 "strain of the two components".

Fixed

124 This equation is based on Glen's flow law, which was never introduced.

Explained that this viscoelastic equation is based on Glen's flow law and added a reference.

124 where does the factor 2 in the first term come from? Using standard Glen's flow law it's just $\varepsilon_{xy} = \boldsymbol{A\tau_E^{n-1}\tau_{xy}}$. Maybe you use non-standard definitions (as compared to glaciology textbooks), but general definitions should be given.

This factor 2 somehow crept in too early and should not be in Eq. 7, however the rest of the Eqs. are correct since, under our assumptions, $\dot{\varepsilon}_{xy} = \frac{1}{2}\frac{du}{dy}$, Eq. 7 has been corrected.

128 usually $\boldsymbol{\tau_E^2 = \frac{1}{2}(\tau_{xy}^2 + \cdots)}$

Since, in the simple case that we outline, τ_{xx}^2 = 0 and $\tau_{yy}^2 = \tau_{zz}^2$, the standard definition for effective stress, i.e.

$$\tau_E^2 = \frac{1}{2}\left(\tau_{xx}^2 + \tau_{yy}^2 + \tau_{zz}^2\right) + \tau_{xz}^2 + \tau_{xy}^2 + \tau_{yz}^2$$

Becomes

$$\tau_E^2 = \frac{1}{2}\left(2\tau_{yy}^2\right) + \tau_{xz}^2 + \tau_{xy}^2$$

And hence leads to equation 9.

133 How is Msf absent? Tidal forcing is mainly vertical.

The Msf frequency is totally absent from the vertical tidal motion, hence why a linear process could not produce it in the horizontal ice flow. We have reworded a sentence in the introduction to emphasise that the Msf frequency is not measurable in the vertical tidal motion.

135 I don't understand how horizontal integration yields a vertical average.

Reworded this to say "integrating with respect to z and y"

Eq 10 explain that s and b refer to surface and bed. Also I think that units don't match since you integrate a stress divided by h (which the bar seems to indicate), to different powers.

Added definitions of s and b, also corrected the typo in Eq. 10.

Eq 17 in the overbrace of the third term: S4 (currently no index)

Fixed

140 and Eq. (10): somehow viscous deformation rates are obtained from elastic stresses, since λ and the τ 's are derived from elastic constants (Eq. (6)). IIUC this should be obtained from the viscous analog stresses with μ = 0.5 (for incompressibility).

As explained above, using a Maxwell rheology the stress is equal in the viscous and elastic components.

175 It would be helpful mentioning why (integration, step from (16) to (17)).

Added this explanation

184 Absolute speedup would also be interesting. IIUC, the relative speedup for small shelves is not due to nshift, but due to an increase of u0.

We intentionally talk about relative rather than absolute speedup because, since all other parameters are kept the same (i.e. we don't change ice viscosity), the majority of absolute speedup occurs for larger shelves because they are less buttressed. Since we want to show how the ice shelf speeds up only due to the n-shift effect, we show the relative speedup compared to the baseline ice shelf velocity with no tides.

185 should this be "Table 1"?

Fixed

191 "dependant" should be "dependent".

Fixed

192 Again, viscous stresses are not the same elastic stresses. The cap on the value of E seems to be a hint in this direction: viscous stresses cannot be much higher for ice rheology since strain-rate softening limits the maximum sustainable stress.

In the Maxwell model, viscous stresses are exactly equal to elastic stresses.

210 Was the model surface geometry prescribed, or free to evolve to a consistent state?

We use a stress-free boundary condition at the ice surface, this BC is now given formally in the relevant section of the model description.

213 Do you mean "Eulerian frame of reference" since total derivatives (Jaumann) appear below? These wouldn't be needed in a Lagrangian frame.

We are slightly confused by this question, firstly total (material derivatives) are different from Jaumann derivatives, and secondly the material derivative is indeed necessary for a Lagrangian frame of reference.

231 give a reference to the Equation how to calculate G in Eq. (22) from E and μ.

Added an in-line equation and reference

Eq 25 why is ρwgwa(t) not included here?

We choose to apply ice shelf stresses rather than ocean pressure, which would instead be appropriate for a calving front (for the Rutford ice stream whose geometry we approximately mimic the GL is very far from the Ronne calving front.

Fig 3 It might be important to highlight that the grounding line is not just upstream, but also sideways of the model.

Done

237 Which physical process generates this buttressing stress?

This term is added to simulate the buttressing downstream of the model domain, caused by lateral stresses not included in the downstream BC. Although it is not necessary, it allows for a relatively uniform ice shelf velocity in the domain (as is observed on the Rutford Ice Stream).

239 and Eqs. (25) and (26): use consistently ρi , or drop the index "i" consistently.

Subscript i is not used at any point for ice density, we use ρ without a subscript for ice density, to avoid confusion when using index notation (i.e. Eq. 19)

240 I have no idea what an "elastic foundation" is. It looks like you just apply a normal stress on all faces in contact with the ocean, or at least this is what it should be. "Elastic" makes no sense here.

Reworded this to avoid confusion. The BC is implemented as an elastic spring foundation and there is an exact mathematical equivalence between ocean pressure and this elastic foundation formulation (e.g. see Gudmundsson 2011).

243 If this corresponds to the green "till" area in Figure 3, please say so.

Done

246 How is this boundary condition implemented? Is a Dirichlet (i.e. velocity) condition prescribed, the magnitude of which is calculated from the basal stress of the last time step solution?

The Weertman style sliding law is implemented by including deformable elements beneath the ice, whose rheology simulates the power sliding law. As such, the surface deformation of these sub-ice elements mimics the basal motion, for a given basal traction. This enables us to solve for basal ice velocity implicitly within the same time step and with the Newton-Raphson method.

256 simply call this section "Discretization"

Done

259 Leave away this sentence, we typically also use HEX20 or even better HEX27, so this is standard.

To our knowledge this type of element is not at all standard in glaciology and so a description is necessary.

260 The model mesh appears extremely coarse for the task at hand. Especially the horizontal discretization in a shear zone should be considerably smaller to resolve the stress concentration there, and the element layer on the sides should be bigger than 2 elements. Or at least some model experiments with double mesh density should be used to show that the chosen resolution is sufficient to resolve the relevant spatial scales. Why was a mesh with such a complicated structure chosen for a block, where a structured mesh, possibly refined in the areas of interest, would have sufficed?

We ran the n3xyz simulation (i.e. the one in which bending stresses generate the largest Msf signal) with double the horizontal mesh resolution and analysed the results. The maximum difference in the Msf amplitude between the two simulations was 3% in the ice shelf shear zone. The maximum difference in ice velocity was 2.5% at the ice shelf front. Apart from these very slight changes in amplitude, the model results were identical. Model run time with this setup increased by an order of magnitude. We have added a comment on this in the new manuscript.
We started with a structured mesh, with a 90 degree angle in the grounding line where the ice ungrounds next the shear margin, but this unnatural grounding line produced larger stresses and we opted to give the mesh a more natural curved grounding line. As a result of this, it became convenient to use an unstructured mesh, however, the elements are only slightly distorted as compared with the structured mesh we began with.

260 Is the mesh moving? If not, how big are the errors in transient stresses?

The mesh is moving

267 ff.: better explain what n1, n3 means, and leave away the "denoted n3xyz" and similar.

Done

268 space missing in x, y, z.

Fixed

Fig 4 It is somewhat confusing to have the horizontal axis reversed as compared to Figures 1 and 3. Better mirror those. Also indicate what is shown with these contours. Are these velocity amplitudes? Or vertical displacement amplitudes at the surface, or the base of the ice? Or horizontal displacements? Additionally, it would help saying that these are map-plane views (I think), of maybe the surface, or average, quantities. Instead of n=1, n=3, the panels should be labeled with the codes of the model experiments e.g. n1xyz. Velocity contours could also be shown for lower velocities, e.g. 0.1, 0.5, 1., 2., such that panels b and c show something interesting

All the above has been implemented into new versions of the figures and figure captions.

288 now this mysterious term is called the "ocean foundation BC", where it was "elastic" in line 240. Just call this the normal stress. Also parenthesis is missing.

Fixed

291 So why FRIS, if everything else, including GPS, is from RIS?

Changed to Ronne Ice Shelf

294 Don't call this "full-Stokes". Either you solve the Stokes equations, or you don't. But here you claim to solve with a viscoelastic rheology, which is again something quite different.

See our reply to the main comment

295 see 294, and please don't perpetuate this stupid "full-Stokes" thing.

See our reply to the main comment

297 Please specify which displacements these are: horizontal or vertical? One would expect to see velocities, given the theoretical section and the model description.

Specified that these displacements are horizontal. We show displacements rather than velocities because, since these are easiest to observe, almost all previous literature discussed tidal effects on ice flow in terms of displacements.

301 "medial line": better write "ice shelf center line"

We feel that medial line is more concise and better gets across that this is a line of symmetry through the entire model.

308 better "For experiment n1xyz …"

Done

323 This scaling makes the comparison with Figure 4 difficult. At least you should indicate the grounded portion on the horizontal scale, this might be estimated to be 0.1? Or even less, since the crosses are the stresses extracted at element centers, or element face centers (actually maybe integration points, unless projected to the nodes)?

The scaling helps make a comparison to the results of section 3. The grounded sidewall is not shown in either figure 4 or 5 (W is defined as the ice shelf half width, not the half width of the entire domain).

325 Since you have symbols, please use those in the descriptions.

Done

327 units of wa = 2 m. But this was already said in line 321.

Added units

328 Don't call yy "longitudinal", this is plain confusing. It is the cross-flow component.

Done

329 where is $\pi/4\lambda$ in the figure? Please help the reader in the figure, or improve the description.

The flexural wavelength lambda, as would be calculated by elastic beam theory (Eq. 6), cannot be directly compared with our model. We could estimate the model lambda from the displacement or stress curves but this does not seem like a useful exercise. Removed the pi/4lambda comment to avoid unnecessary complication.

333 Probably first tell the reader that τxy is the boring component holding back the weight of the ice, that you would get irrespective of rheology.

This is pointed out earlier in the paper

333 Also show, and discuss, τE, this is the main point of the paper.

Effective stress added to Fig. 5 and new Fig. 6, with discussions added.

335 again, no full-Stokes. And as said just above, this part is boring since you get that with any rheology, it's just force balance.

As we state at its start, the point of this paragraph is to check some of the assumptions in section 3, one of which was that tau_xy varies linearly with distance from the sidewall.

Fig 5 Indicate the grounded part with a colored bar along the horizontal axis, or a vertical dotted line, or similar. Also plot the effective stress, since this is the quantity that is crucial for the whole argument.

None of this figure shows results on grounded ice. Effective stress has been added

334 This section should go to the discussion.

In principal we agree but this is short and flows nicely where it is, whereas it's difficult to see where to put it into the discussion where it doesn't break up the flow.

336 Why is τxx increasing downstream? Is this already the effect of the end of the domain, or the standard ice shelf extensional stress?

These are standard ice shelf extensional stresses, which begin to dominate away from the sidewall, added a comment on this.

340 again, why full-Stokes? This is visco-elastic!

See our reply to the main comment

348 No, you have not shown that, at least not in the paper. Why aren't any plots of the velocity-spectrum, together with the forcing, shown. Or at least curves of the time-variation of forcing and response. After reading on I found Figure 6 which sort of shows this. So why is this not presented in the "Results" section, such that it could be meaningfully discussed?

The amplification of the Msf signal downstream of ice stream GLs is shown in the results section in figure 4a and this point is made in the paragraph that presents these results at the start of the section.

355 I sincerely doubt this claim when using a spatial resolution of only 300 m. This effect might be quite important, but will be smoothed out by the horizontal and vertical approximation functions.

Quadratic elements can capture this across-flow velocity profile very nicely, tests with double mesh resolution produced a very similar number.

362 This period-doubling has been nicely shown in the theoretical part, although with some doubts concerning the problem with viscous/elastic stresses. Now one would like to see this frequency-doubling also in the FE model results. So it would be very nice to have a plot with forcing and response at different points on the domain. Maybe the argument is that the stresses are highest at high tide, and therefore viscous deformation rates. But since everything is transient, and you have a viscoelastic membrane that is bent up and down, there must be location dependent delays.

This figure has been added

362 Why at high and low tide? Vertical velocities are highest during rising and lowering. You could/should investigate this claim by just extracting the second invariant from your transient model runs.

This is now shown in figure 6 and the phasing discussed

365 "medial line"

See earlier response

Fig 6 It is not clear what is shown in this figure. Is this the FFT (frequency spectrum) of the model response? What was the strength of the forcing? It would be very helpful to also show the time series. Panel (b) should be labeled with (m/d), as it shows velocities. Panel (c) (missing) should show the effective stress in the shear margin. This figure would also be a good place to compare the results from the three model runs, maybe as colored bars.

The figure is now introduced more clearly, explaining exactly what it shows. The suggestion for panel c has been included in a new figure.

371 "…than the run time of 60 days".

Changed to "are not resolvable with a simulation time of sixty days"

375 I think this is "vice versa" (good old Latin).

Fixed

402 Again, no "full-Stokes".

See our reply to the main comment

414 Add some discussion of additional, state-changing processes here (see general comment).

Added a new paragraph discussing these processes

Reply to Victor Tsai

Major Comments:

In reality, the grounding line does not act like a fulcrum and is not fixed. Although the authors have discussed the possibility of grounding line migration somewhat, they have not discussed whether the bending stresses simulated near the grounding line might be overestimated because of the lack of migration (which alleviates the need of the grounding line to bend somewhat). Because the grounding line is assumed to be pinned ("clamped"), they cannot evaluate the possibility that asymmetries in grounding line migration may produce a strongly nonlinear ice shelf flow response (as in Robel et al. 2017, see later comment). This fixed nature of the assumed grounding line therefore seems to be a very important difference between the simulation result with reality, and must be discussed. At a minimum, the authors should describe why they expect their modeling framework to still be useful despite the simplifications.

This point raises two separate issues: overestimating the magnitude of bending stresses and the potential role of GL asymmetry to generate an Msf signal, and so we address each in turn. Firstly, regarding bending stresses, although it is not mentioned in the manuscript we tested whether allowing the GL to migrate (for a steep bed slope) had a major impact on the magnitude of bending stresses and this was not the case. For a positive vertical tidal motion of 2m, effective stress at the pinned GL node was 67% greater than for the migrating case, however this large stress is highly localised and the depth averaged effective stress at the grounding line is only 12% greater for the pinned GL. The differences in stress will have some impact on the strength of the mechanism described, but we do not think this error to be any worse than other simplifications such as an isotropic rheology and lack of damage in the shear margin. We have added a discussion on this issue in the revised manuscript. On the second point, as we mention in the manuscript, we intentionally do not allow the GL to migrate in order to isolate the nonlinear rheological mechanism that we are proposing from this alternative mechanism. Since there is currently no strong evidence of GL migration in this area and bed slopes around the GL are not known, it would be difficult to properly model this effect anyway. Also, GL asymmetry was first proposed (and modelled in some detail) as a mechanism a few years previously (see section 3.2 of Rosier et al., 2014).

2. It is a basic mathematical fact that a nonlinear process forced at more than one frequency will produce a response at harmonics and beats of those frequencies. The authors claim later in the paper that the flexure mechanism is the only way to produce the M4 response, but they have not proven that other nonlinear processes could not produce such a response. Indeed, Robel et al. 2017 makes this exact point in their equations 11-13. Which brings up the next point. . .

We absolutely agree with the point made here, certainly any nonlinear process will produce other frequencies as we discuss in the paper. This needed to be made clearer in our manuscript and we are not trying to claim that this mechanism is the only one capable of producing these high frequencies. Our argument is that there should be a large difference in the amplitude of the response in ice velocity at these higher frequencies that could help diagnose which mechanism is at play. In the Robel (2017) mechanism, the primary response over one tidal cycle is to increase velocity at high tide and decrease velocity at low tide. As the reviewer points out, other frequencies will be in the velocity waveform because the response is nonlinear. However, in the mechanism we put forward, the primary response over one tidal cycle will be to increase velocity twice during one tidal cycle (i.e. precisely at the higher frequencies), and so the high frequencies can be expected to be of much larger

amplitude. In this way, observations of a strong velocity response at these frequencies would be evidence that this mechanism is playing an important role. The main point we are raising, therefore, is that while all non-linear processes can give rise to M4, MS4, Msf etc. the ratios of those amplitudes will, in general, be different. Now that we have seen the alternative mechanism put forward by Robel et al. 2017 we can compare the relative strength of the frequencies generated and this reveals that the dominant frequencies generated in ice shelf velocities are M2 and S2. Since our analysis of RIS ice shelf velocities finds the MS4/M4 frequencies dominate, as in our mechanism, we think this is compelling evidence that the flexural ice-softening mechanism is primarily responsible for the observed Msf response on Rutford. We do realize that in our original manuscript much of this was not particularly well articulated, and we have largely re-written this section in order to get our point across more clearly.

3. There needs to be much more engagement throughout this paper with the arguments put forward by Robel et al. 2017. While we recognize that this paper was published near the time of submission of the current manuscript, the fact that the article discusses so many of the same issues, including many of the main points of the present manuscript, while also proposing a different basic mechanism related to asymmetries in contact stress from asymmetric grounding line migration, obliges the authors to discuss the Robel et al. paper and contrast their work with that work. For example, at a number of points, it is claimed that the tidal flexure mechanism is the only way to produce an increasing Msf signal in the shelf, which is also what Robel et al. 2017 claims, and the authors also claim that previous models do not reproduce observations in floating ice shelves (which is not true anymore due to the Robel work). Lines 25, 36, 155-160, 295-300, and all of the discussion and conclusions therefore need modification to be accurate and to appropriately cite the present literature.

We have added discussions of the Robel 2017 paper throughout, as is appropriate since we are investigating the same problem but come to very different conclusions (incidentally we did not see a copy of the Robel 2017 paper before submission, as can be easily verified by comparing the dates of submission/publication).

4. (Lines 357-361 and elsewhere) What about Msf signals generated in the grounding line and then propagated downstream throughout the shelf? Wasn't this the previous explanation for the ice shelf Msf signal? Something that is not remarked upon in this paper in the temporal phasing of signals, which is important given than the Msf signal appears first in the ice shelf.

The assumption previously (before the Minchew 2016 satellite observations) has been that the Msf signal was generated upstream of the grounding line (due to a nonlinear sliding law and/or subglacial drainage processes). The Minchew 2016 observations show the phase leading on the ice shelf, and this is replicated in our model. We have added a remark on this point in the discussion. We have also included a figure showing more details of the phasing.

5. I agree that the elastic response can only ever yield a linear response. However, the elastic response can potentially produce a large signal at the primary tidal frequencies. The authors should at least provide an argument (in the analytic section) as to why the elastic deformation is small and so can be neglected in the analytic section.

We do not understand the point being made here. We all agree that the elastic part of the Maxwell model can only yield a linear response and we explain in the same paragraph that we are concentrating on the nonlinear response because this is the only thing that can explain the observed Msf signal. We are hence not neglecting the elastic deformation but simply using the fact that the

linear response cannot generate any Msf signal and does therefore not need to be considered in this particular case.

6. It is clear from the difference between n3xyz and n3xy experiments that confinement plays an important role in producing the Msf signal at an amplitude comparable to that observed at the RIS shelf. What about unconfined shelves? Does this indicate that such shelves should have much less Msf response? What about Bindschadler and the other FRIS ice streams? For example, does this imply that the proposed mechanism does not explain the observations of a significant Msf response at Bindschadler. Also, it would be good to state, early on, that Rutford Ice Stream goes afloat in a trough and remains in that trough, for perhaps ~100 km downstream of the grounding line. A map of ice velocities (like Figure 1b of Minchew 2016) would help put this in context.

In an unconfined ice shelf (such as an ice tongue) our proposed mechanism would still produce an Msf signal at the main GL, and since there would be no sidewall friction the amplitude of this signal would not decay downstream, unlike in our n3xy simulation. Certainly this mechanism will be strongest for very confined ice shelves of which the outlet of Rutford is a good example but many others exist, for example Evans and Foundation Ice Streams. The Msf response at Bindschadler is far smaller than is observed on the FRIS ice streams (because the semidiurnal tides are of low amplitude) and it seems that this could be easily produced by bending stresses at the GL but it is possible that the pinning point downstream plays a role. Determining this would require more observations, together with accurate measurements of bed slopes and/or migration distances.

7. One aspect of the Minchew 2016 observations that are not explained by this model is the along-flow variation in strain rate in the ice shelf. That study invokes a possible pinning point to produce such heterogeneity. Perhaps this should at least be remarked upon.

Our mechanism could in fact produce heterogeneity in any number of ways, through variations in ice properties. The ice rheology in our model is kept intentionally homogeneous to avoid complicating the interpretation and although we use a very simplified Rutford geometry our goal is not to reproduce these observations or indeed discuss them to any great length. That being said, the heterogeneity is interesting and we have added a discussion on this.

Minor Comments:

Line 16-17: Please rewrite for clarity: "the primary ice flow response is at a different frequency than the highest amplitude frequency of tidal forcing"

Changed to "on the Rutford Ice Stream (RIS) the primary response is at a fortnightly (Msf) frequency that is not measurable in the vertical tidal motion"

Line 26-27: Awkward sentence phrasing

Reworded

Line 30: rheological behavior and the response to external forcing

Added this to the end of the previous sentence

Line 79-81: Would be useful if this sentence came much earlier to direct focus to the figure

Done

Line 122: There are not separate viscous and elastic stresses. There is simply one stress which causes both viscous and elastic deformation. This sentence therefore should be rewritten to clarify.

Reworded this sentence to clarify

Equation 10: This is clearly only do-able in this way for n=3. Could you use a perturbation approach (or expand about \tau_xy) to solve for general n?

This would be an interesting future extension to the work, as we mention at the end of the paper it could be possible to infer a value for 'n' from observations of this nonlinearity and so understanding how different values of 'n' produce different frequencies would be important. For now, since 'n=3' is a very standard assumption in glaciology, we prefer this simpler approach since it only produces one set of frequencies and is easier to interpret.

Line 176: How large are the linear elastic and damming stresses in comparison to the nonlinear viscous changes that you are simulating?

In this section we explore the flexural ice-softening mechanism in isolation, to simplify the analysis, and do not include these terms. Both of these effects are included in our 3D model, and we have added a comment pointing this out in this sentence.

Line 231: It needs to be explained more clearly why the elastic modulus in the analytic calculation has to be so different from the numerical calculation. (Why does this produce such high bending stresses in the analytic case?)

We have reworded this paragraph to explain this better.

Line 240: What is an elastic foundation? Perhaps use a clearer term.

Changed to normal stress

Line 245-250: Should say why you can be sure that the nonlinear sliding law isn't producing the Msf response. (I can see that it isn't because all the numerical experiments use the same sliding law.) Also, the authors should comment about what this implies about the results in Gudmundsson 2007, 2011 and other studies. . .

We have added several sentences in the discussion which cover this

Figure 4: Msf amplitude in what quantity? (same comments for line 298)

Expanded on this description (Msf amplitude in horizontal surface ice displacements)

Line 303-308: Should state outright here that the amplitude of Msf response is an order of magnitude less than in the n3xyz experiment.

In fact the Msf amplitude at the main GL is more or less the same as the n3xyz experiment (since bending stresses are generated here), we have changed the wording of this paragraph to clarify how the Msf amplitude compares to the n3xyz experiment.

Line 327: units of w_a?

Added units (m)

Line 367: Would the response at M2 and S2 frequencies be larger if the elastic modulus was different? The relative difference between linear elastic and nonlinear viscous responses will be a strong function of the relative size of viscosity and elastic modulus.

The linear elastic response, which will largely consist of M2 and S2 frequencies, would undoubtedly be larger if the elastic modulus was different. However, the elastic modulus is not a tuneable parameter, its value is set in order to match a Burgers rheology at tidal frequencies, as in Gudmundsson 2011.

Line 408: Remove "to this day"

Done

At the end of this file we have included a marked-up manuscript showing changes to the paper. Please note that some reviewer comments were implemented to the originally submitted .tex file before a new version was created and so not every single change is highlighted in red, however the majority are shown. Our apologies for this oversight, we hope that the marked-up version can still serve as a useful guide to highlight the main changes.

Manuscript prepared for The Cryosphere
with version 2014/09/16 7.15 Copernicus papers of the LaTeX class copernicus.cls.
Date: 9 March 2018

Tidal bending of ice shelves as a mechanism for large-scale temporal variations in ice flow

Sebastian, H. R. Rosier[1] and G. Hilmar Gudmundsson[2]

[1]British Antarctic Survey, High Cross, Madingley road, Cambridge, UK
[2]Department of Geopgraphy and Environmental Sciences, Northumbria University, Newcastle-upon-Tyne, NE1 8ST, UK

Correspondence to: S. H. R. Rosier (s.rosier@bas.ac.uk)

Abstract. GPS measurements reveal strong modulation of horizontal ice-shelf and ice-stream flow at a variety of tidal frequencies, most notably a fortnightly (M_{sf}) frequency not present in the vertical tides themselves. Current theories largely fail to explain the strength and prevalence of this signal over floating ice shelves. We ~~propose that tidal bending stresses, through the nonlinear rheology of glacier ice , can have a sufficiently large impact on the effective viscosity of ice along its floating margins to~~ show how well-known nonlinear aspects of ice rheology can give rise to ~~significant and widespreadtemporal variations in the horizontal velocity of ice shelves~~widespread, long-periodic tidal modulation in ice shelf flow, generated within ice shelves themselves through tidal flexure acting at diurnal and semi-diurnal frequencies. Using full-Stokes viscoelastic modelling, we show that inclusion of tidal bending within the model accounts for much of the observed tidal modulation of ice-shelf flow. Furthermore, our model shows that, in the absence of vertical tidal forcing, the mean flow of the ice shelf is reduced by almost 30 % for the geometry that we consider.

1 Introduction

Ocean tides are known to greatly affect the horizontal flow of both ice shelves and adjoining ice streams, even far upstream of grounding lines (GLs) (**?????????????**). In some cases the horizontal ice flow responds at a different frequency to the tidal forcing, for example on the Rutford Ice Stream (RIS) the primary response is at a fortnightly (M_{sf}) frequency that is not measurable in the vertical tidal motion (**?**). More recent observations have shown that the M_{sf} signal actually increases in strength on the adjoining ice shelf (**??**) and also exists on isolated ice shelves which do not have large ice streams feeding into them (**??**).

A multitude of mechanisms have been proposed which could lead to a fortnightly modulation in ice flow: a nonlinear basal sliding law (**???**), tidal perturbations in subglacial water pressure (**??**), ~~GL~~ grounding line migration (**??**) and changes in the effective ice-shelf width (**?**). ~~Understanding the root cause of the strong and widespread tidal signals observed on~~ Identifying the mechanism whereby ocean tides generate the observed tidal modulation in ice flow is important for several reasons. The amplitude of these perturbations is often a significant fraction of mean flow speed and the perturbations are widespread, impacting ice flow on a large number of ice streams and several ice shelves. Not knowing the root cause of these tidal modulations therefore implies a significant lack in our understanding of the forces controlling the large scale ice flow of the Antarctic Ice Sheet. Furthermore, there are good reasons to believe that the tidal response is significantly affected by the rheology of ice or mechanical conditions at the base of ice streams, or possibly both in combination. Hence, once the mechanism has been fully identified, one can expect to be able to make inferences about ice ~~shelves and ice streams provides unique insights into their response to external forcing. The periodic and predictable nature of the ocean tide, together with the complexity of the observed response, means that tides act as a natural experiment with which we can learn about how ice flows andits time-dependant rheological behaviour~~rheology and/or basal conditions from observations of tidal modulations in ice flow. The Filchner-Ronne Ice Shelf (FRIS) is a particularly good natural laboratory for obtaining these insights because of the considerable tidal range, which can be as large as 9 m (**?**).

Previous modelling studies have focused almost exclusively on tidal modulation of ice-stream flow (**?????????**), whereas tidal modulation of the flow of ice shelves has received much less attention. This is possibly because it has often been assumed that the M_{sf} signal observed on ice shelves is driven by processes occurring on neighbouring ice streams; indeed these make up the bulk of the proposed mechanisms listed above. Now that new observations show the M_{sf} signal strengthening downstream of GLs (**??**) it has become clear that an alternative mechanism is needed which can generate this signal, independent of anything occurring on grounded ice (**???**).

Here, we will show how the observed widespread tidal modulation in ice flow can be generated within ice shelves themselves through tidal flexure. We begin with a description of this simple mechanism, which results directly from the well-known nonlinear aspect of the flow law of glacier ice and hence does not require an ice stream to act as a source of the observed tidal signals. Then in Sect. 3, using elastic beam theory, we derive a simple mathematical description of this mechanism that yields some insights into its importance for various ice-shelf configurations. Finally in Sect. 6, we present results from a 3-D full-Stokes viscoelastic model of a confined ice shelf, with a similar geometry to the RIS, that incorporates the new mechanism and is capable of replicating many of the observed characteristics of the tidal response of the Ronne Ice Shelf. These results will show that this mechanism has important implications for both the time-varying and mean flow of ice shelves subjected to strong vertical ocean tides.

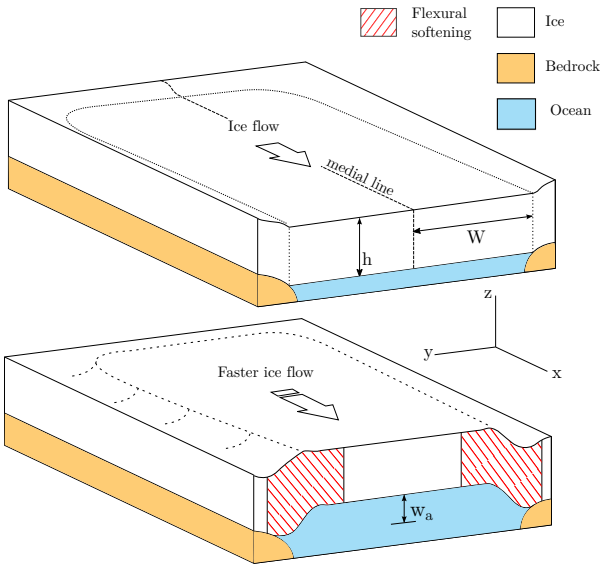

Figure 1. Schematic showing the flexural ice-softening mechanism for a confined shelf, together with the geometry of the problem described in Sect. 3. The top panel shows the situation with no tidal uplift and the bottom panel shows how ice flow is enhanced as ice is softened in the shear margins due to flexural stresses generated by a vertical tidal motion (w_a).

2 Flexural ice-softening mechanism

The Filchner-Ronne, Larsen and to a lesser extent Ross Ice Shelves are situated in tidally energetic regions, and thereby subjected to large vertical motion at tidal frequencies. By far the largest tidal amplitudes are in the Weddell Sea region, particularly at the grounding line of large ice streams such as Rutford and Evans (**?**). In the grounding zone (here defined as a band along the grounding lines that extends several kilometers into the main shelf) the ice bends to accommodate these large vertical tidal motions. This bending generates longitudinal and shear stresses within the ice which contribute to the effective stress and are strongest near the grounding line during high and low tide. Since ice is a non-Newtonian shear thinning fluid its effective viscosity will be altered by these tidal stresses. ~~Specifically, just before peak high and low tide the effective ice viscosity will be reduced compared to the situation with no vertical tidal motion.~~ A schematic showing how vertical tidal motion can lead to a reduction in effective viscosity of ice shelf shear margins is shown in Fig. 1. This effect, which we will call 'flexural ice-softening', leads to an increase in ice velocity during high and low tide. ~~This is simply a~~ We will show that this is a direct consequence of the nonlinearity of Glen's flow law.

Since it is the magnitude of stresses and not their sign that contributes to the effective viscosity, there is no difference in the flexural ice-softening effect between high and low tide. The only time

that the effective viscosity of an ice shelf subjected to large tides will increase to that of an ice shelf without tides is when the vertical deflection is small, i.e. between high and low tide or during neap tides. As a consequence there are two other important repercussions for the ice-shelf flow that arise from this mechanism, aside from the direct increase in velocity at high and low tide. Firstly, the mean flow of an ice shelf is greater in the presence of large tides because, even at its slowest, it will be flowing at least as fast as an ice shelf without tides. Secondly, because the change in velocity (due to ~~effective~~ flexural ice- softening) during spring tide is ~~much~~ larger than during neap tide, the ~~ice shelf~~ ice-shelf flow will be modulated at an M_{sf} period (provided the rheology is nonlinear, as is the case for glacier ice). Since many large ice shelves are confined on three sides by grounded ice, the bending stresses are generated along their entire length. This mechanism could therefore explain how the M_{sf} signal increases in strength downstream of ice stream grounding lines, as evidenced by recent GPS and satellite observations (**??**).

3 Analytical solution for flexural ice-softening

Elastic beam theory provides a useful starting point for evaluating the magnitude of these tidal bending stresses on an ice shelf and their impact on its effective viscosity. We start from a simple confined ice shelf whose geometry is invariant across flow (in the y direction) and with a constant thickness gradient in the down-flow x direction. The ice shelf is symmetrical about the centerline, which is distance W from the two sidewalls at $y = 0$ and $y = 2W$ (Fig. 1). For this analytical solution we assume that the portion of the ice shelf that we investigate is sufficiently far from the GL that the only bending occurs across-flow. The situation near the main GL of a narrow confined shelf will be a complex combination of along and across-flow stresses that we shall ignore for now. Deviatoric stresses are defined as

$$\tau_{ij} = \sigma_{ij} - \delta_{ij}\sigma_{kk}/3 \tag{1}$$

where σ_{ij} are the components of the Cauchy stress tensor, δ_{ij} is the Kronecker delta and $p = -\sigma_{kk}/3$ is the isotropic pressure. We use the comma to denote partial derivatives and the summation convention, in line with standard tensor notation.

We immediately make the simplifying assumptions (motivated by full-Stokes calculations presented below) that $\tau_{xx} = \tau_{xz} = 0$, hence $\tau_{yy} = -\tau_{zz}$, $\sigma_{zz} = -p - \tau_{yy}$ and $\sigma_{xx} = -p$. Furthermore, we assume that the only important contributions to τ_{yy} and τ_{yz} are due to tidal bending. The force balance equations in x and z reduce to the following form:

$$-\partial_x p + \partial_y \tau_{xy} = 0 \tag{2a}$$

$$\partial_y \tau_{yz} + \partial_z \sigma_{zz} = \rho g \tag{2b}$$

Note that in this system σ_{zz} is not cryostatic, unlike in the shallow shelf and shallow ice approximations. We are interested in finding an expression for the across-flow variation in downstream velocity,

$u(y)$, for which we need an expression for τ_{xy}. As we show in appendix A, τ_{xy} is essentially independent of the tidal stresses (as well as x and z) and can be approximated by

$$\tau_{xy} = F_d h (W - y), \tag{3}$$

where $F_d = \rho g \partial_x s$.

Linear elastic beam theory gives us an expression for the elastic stresses that will arise due to tidal bending (**?**). Although strictly derived for an infinitely long ice shelf, we show in appendix B that the equations in **?** provide a good approximation for the geometry that we are interested in. The two contributing stresses, related to the bending moment and its derivative, are the across-flow longitudinal bending stress:

$$\tau_{yy} = \frac{-6 w_a \rho_w g z}{h^3 \lambda^2} e^{-\lambda y} \left[\cos(\lambda y) - \sin(\lambda y)\right] \tag{4}$$

and the across-flow shear bending stress:

$$\tau_{yz} = \frac{6 \rho_w g w_a}{h^3 \lambda} e^{-\lambda y} \cos(\lambda y) \left[\frac{h^2}{4} - z^2\right], \tag{5}$$

where

$$\lambda^4 = \frac{3 \rho_w g (1 - \mu^2)}{E h^3}, \tag{6}$$

w_a is the vertical tidal motion, E is the Young's modulus of ice, μ is the Poisson's ratio and ρ_w is the density of seawater. The vertical coordinate, z, is defined as the vertical distance above the neutral axis of the ice shelf, which we assume to be halfway through its thickness.

At this stage we employ a Maxwell rheological model consisting of a linear elastic spring and a nonlinear viscous dashpot, whose behaviour is modelled by Glen's law (**?**), connected in series. With this viscoelastic model the total strain is the sum of the viscous and elastic strains and the stress is equal in the two components. In this way, we can express the horizontal shear strain rate as

$$\dot{\epsilon}_{xy} = 2A A \tau_E^{n-1} \tau_{xy} + \frac{1}{G} \frac{1}{2G} \dot{\tau}_{xy} \tag{7}$$

where

$$G = \frac{E}{2(1 + \mu)} \tag{8}$$

and, based on the assumptions given above,

$$\tau_E \approx \sqrt{\tau_{yy}^2 + \tau_{xy}^2 + \tau_{yz}^2}. \tag{9}$$

Motivated both by our findings in the appendix that $\dot{\tau}_{xy} \approx 0$, and by the fact that this elastic term can only ever yield a linear response to the tidal forcing, we discard it and focus only on the nonlinear viscous response. We are concentrating on the nonlinear response because only this can explain

modulation of horizontal ice-shelf flow at an M_{sf} frequency, given that the M_{sf} constituent is absent in the vertical tidal forcing.

By assuming that $n = 3$, we can separate the velocity into unperturbed and time-varying components. Integrating with respect to z and y then gives the depth averaged velocity $\overline{u}$ as

$$\overline{u}(y,t) = \frac{2A}{h}\left(\overbrace{\int_0^y h\overline{\tau_{xy}}^3 dy}^{u_0} + \overbrace{\int_0^y h\overline{\tau_{xy}}\int_b^s \tau_{yy}^2\, dz dy}^{u_{\text{long}}} + \overbrace{\int_0^y h\overline{\tau_{xy}}\int_b^s \tau_{yz}^2\, dz dy}^{u_{\text{shear}}}\right) \tag{10}$$

where s is the surface, b is the bed and $\overline{\tau_{xy}}$ is the depth averaged shear stress. We have split this into the three components, denoted as the unperturbed (u_0), long(itudinal) bending stress and shear bending stress contributions to ice flow. Evaluating the integrals for each term and neglecting the overbar since everything is now depth averaged yields:

$$u_{\text{long}} = \frac{3AF_d(\rho_w g w_a)^2}{2h^4\lambda^6}\left[e^{-\gamma}\left(1 - 2\xi + \xi\sin(\gamma) + \cos(\gamma)\left[\xi - \frac{1}{2}\right]\right) + \lambda W - \frac{1}{2}\right] \tag{11}$$

where $\xi = \lambda W - \frac{\gamma}{2}$ and $\gamma = 2\lambda y$,

$$u_{\text{shear}} = \frac{3AF_d(\rho_w g w_a)^2}{10h^2\lambda^4}\left[e^{-\gamma}\left(1 - 2\xi - \xi\cos(\gamma) + \sin(\gamma)\left[\xi - \frac{1}{2}\right]\right) + 3\lambda W - 1\right] \tag{12}$$

and

$$u_0 = \frac{1}{2}AF_d^3\Big(W^4 - (W-y)^4\Big). \tag{13}$$

The shear and across-flow longitudinal components can be combined, such that the total (time-varying) velocity $u = u_0 + \Delta u$. Along the centerline at $y = W$, the change in velocity due to tides (Δu) is

$$\Delta u = w_a^2 B, \tag{14}$$

where

$$B = \frac{3AF_d\rho_w^2 g^2}{2h^2\lambda^2}\left(e^{-\gamma}\left[\frac{1}{5} - \frac{\sin(\gamma)}{10} + \frac{1}{h^2\lambda^2} - \frac{\cos(\gamma)}{h^2\lambda^2}\right] + \frac{3\lambda W}{5} - \frac{1}{3} + \frac{W}{h^2\lambda} - \frac{1}{2h^2\lambda^2}\right) \tag{15}$$

To illustrate the consequences of a typical tidal action for the ice-shelf flow, we assume that the time-varying sea level $w_a(t)$ can be written as the sum of two cosines of amplitude a_{M_2} and a_{S_2} and angular frequency ω_{M_2} and ω_{S_2}, i.e.

$$w_a(t) = a_{M_2}\cos(\omega_{M_2}t) + a_{S_2}\cos(\omega_{S_2}t). \tag{16}$$

These two cosines represent the principal lunar (M_2) and solar (S_2) semidiurnal tides, which dominate in the area of interest. Crucially, because the velocity is a function of tidal deflection squared,

new frequencies emerge which, if we assume it takes the form of Eq. 16, expands as follows:

$$w_a^2 = \frac{a_{M_2}^2 + a_{S_2}^2}{2} + \overbrace{\frac{a_{M_2}^2}{4}\cos(2\omega_{M_2}t)}^{M_4} + \overbrace{\frac{a_{S_2}^2}{4}\cos(2\omega_{S_2}t)}^{S_4} + \overbrace{\frac{a_{M_2}a_{S_2}}{2}\cos(\omega_{MS_4}t)}^{MS_4} + \overbrace{\frac{a_{M_2}a_{S_2}}{2}\cos(\omega_{M_{sf}}t)}^{M_{\mathrm{sf}}}, \quad (17)$$

where $\omega_{M_{sf}} = \omega_{S_2} - \omega_{M_2}$ and $\omega_{MS_4} = \omega_{M_2} + \omega_{S_2}$. The four emergent frequencies that we expect to see are labelled according to their respective tidal constituent names. Depending on the relative size of the M_2 and S_2 vertical tidal forcing, different frequencies will dominate in the horizontal ice flow response. In the case of the Filchner-Ronne Ice Streams, the amplitude of the S_2 constituent is typically about half that of the M_2 constituent. As a result, the S_4 frequency will be much smaller than the other three. In terms of velocities, the amplitudes of the M_{sf} and MS_4 components will be equal, and larger than the M_4 component as long as $a_{S_2} > a_{M_2}/2$. ~~We explore this in more detail later.~~

Several useful results are now easily obtained with Eqs. 17 and 14, for example the amplitude of the M_{sf} component in ice-shelf velocity is simply $(Ba_{M_2}a_{S_2})/2$. Integrating with time gives an expression for displacements, which are more readily measured with in-situ GPS. Once again, the amplitude of the M_{sf} component in displacements in this case becomes $(Ba_{M_2}a_{S_2})/2(\omega_{S_2} - \omega_{M_2})$. Even more interesting is the result of the first term of Eq. 17, which acts to increase the time-averaged ice-shelf velocity (u_{mean}). The size of this effect, which we call the n_{shift} is given by

$$n_{\mathrm{shift}} = \frac{B(a_{S_2}^2 + a_{M_2}^2)}{2}, \quad (18)$$

such that $u_{\mathrm{mean}} = u_0 + n_{\mathrm{shift}}$. Interestingly, within this framework all tidal energy at the original (vertical) semidiurnal forcing frequencies disappears (as can be seen by squaring the tidal forcing, Eqs. 16–17). In reality linear elastic effects and changes in damming stresses would be expected to produce some response at these frequencies and these terms are included in the 3-D model described in Section 4. Note that from Eq. 10 onwards these results have been derived under the assumption that $n = 3$. For $n = 1$ bending stresses have no impact on the ice-shelf viscosity and so the M_{sf} flow-modulation and n_{shift} would be identically equal to zero.

Using the simple set of equations outlined above we can easily explore the parameter space to see how the strength of the tidal response changes. Of particular interest is how the n_{shift} leads to an increase in the mean speed of the ice shelf. In Fig. 2 we show speed-up along the ice shelf medial line (solid black contour) as a percent of the baseline speed with no tides, i.e. u_{mean}/u_0 (the parameters chosen are shown in Table 1). This shows that, for a given tidal amplitude, the n_{shift} effect will be most strongly felt on a narrow, thin ice shelf. Conversely, the amplitude of the M_{sf} signal in ice shelf displacements (dashed contour) is strongest for wide, thick ice shelves. The apparent discrepancy is

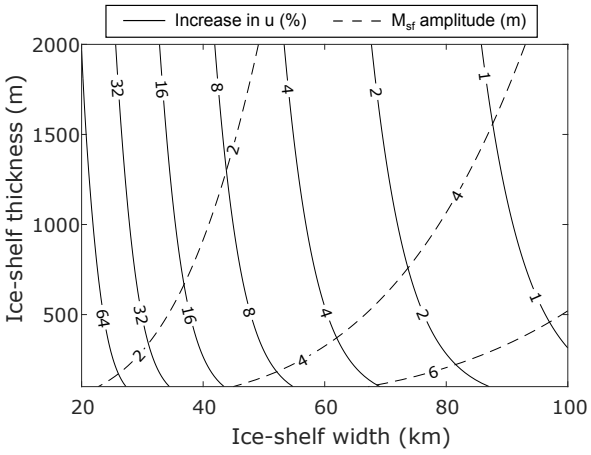

Figure 2. Contour plot of ice-shelf speed up due to tides, as a percent of the baseline speed, predicted by the analytical solution in Eq. 18. Speed-up is predicted along the ice shelf medial line using parameter values given in table 3. Also shown are contours of the amplitude of the M_{sf} signal in ice-shelf displacements (dashed contours).

because, with all other parameters held constant, a wider ice shelf will flow much faster and so the increase in speed as a percent of the baseline is much less.

Note that we use a different value of E in this analytical solution than for our full-Stokes model. ~~In reality, the Young's Modulus of ice is frequency dependent and using the~~ Using the instantaneous Young's modulus of 9 GPa (suggested by laboratory experiments) ~~will~~ would result in bending stresses that are ~~far~~ too large. ~~Instead, we~~ This is because ice behaves viscoelastically at tidal frequencies and E is frequency dependent. Since the elastic beam model we use cannot capture this complexity then instead we treat this value as a tuning parameter and pick a value of E that best matches our modelled bending stresses, which turns out to be 800 kPa.

4 Full-Stokes Model Description

In order to explore the idea of flexural ice-softening in more detail, we undertook modelling experiments on an idealised ice stream/shelf domain using the commercial finite element software MSC.Marc, which has been used extensively in the past to explore the tidal response of ice streams (**????**). The idealised ice stream is 28km wide (to match the approximate average width of the RIS) and consists of a 150 km floating shelf and 80 km grounded ice (Fig. 3). Although data now exists showing tidal modulation on other ice streams, the RIS lends itself well to an idealised study of this kind because of its relatively simple geometry and because its flow has remained largely unchanged over the measurement period (**?**). Surface and bed slopes of the ice stream and ice-shelf portions of the model are approximate averages of the slopes found on RIS, and ice thickness at the downstream limit of the domain is 1420 m. The model is run forward in time for 60 days in order to resolve the

Table 1. Choice of parameters used in Eq. 18 to produce Fig. 2.

Parameter	Value	Unit
n	3	-
a_{M_2}	1	m
a_{S_2}	1	m
ρ	910	$\mathrm{kg\,m^{-3}}$
ρ_w	1030	$\mathrm{kg\,m^{-3}}$
g	9.81	$\mathrm{m\,s^{-2}}$
μ	0.3	-
E	800	kPa
$\partial_x s$	5e-4	-

M_{sf} signal. The grounding line position is fixed and cannot migrate at tidal frequencies, since our focus is only on the effects of tidal bending stresses. We investigate several test cases (Sect. 5), some of which require a slightly different model set up, which we describe in the relevant sections.

4.1 Field Equations

The full-Stokes solver MSC.Marc uses the finite element method in a Lagrangian frame of reference to solve the field equations:

$$\frac{D\rho}{Dt} + \rho v_{i,i} = 0, \tag{19}$$

$$\sigma_{ij,j} + f_i = 0, \tag{20}$$

$$\sigma_{ij} - \sigma_{ji} = 0, \tag{21}$$

representing conservation of mass, linear momentum and angular momentum, respectively. In the above equations, D/Dt is the material time derivative, v_i are the components of velocity, σ_{ij} are the components of the stress tensor, ρ is the ice density and f_i are the components of the gravity force.

We use a nonlinear Maxwell viscoelastic rheology in a slightly modified form to Eq. 7, which can be written as

$$\dot{e}_{ij} = \frac{1}{2G}\overset{\triangledown}{\tau}_{ij} + A\tau_E^{n-1}\tau_{ij}, \tag{22}$$

where the full stress tensor contributes to the effective stress, i.e.

$$\tau_E = \sqrt{\tau_{ij}\tau_{ji}/2} \tag{23}$$

and the superscript $\triangledown$ denotes the upper-convected time derivative:

$$\overset{\triangledown}{\tau}_{ij} = \frac{D}{Dt}\tau_{ij} - \frac{\partial v_i}{\partial x_k}\tau_{kj} - \frac{\partial v_j}{\partial x_k}\tau_{ik} \tag{24}$$

(**?**). We use the same rheological parameters as in **?**, which are found to replicate the behaviour of the more complex Burgers model at tidal frequences, i.e. $E = 4.8$GPa and $\mu = 0.41$, where $E = 2G(1+\mu)$ (**?**).

4.2 Boundary Conditions

At the downstream limit of the domain we prescribe the ice shelf stresses:

$$\sigma_{xx} = -\rho g(s-z) + \frac{\rho g h}{2}\left(1 - \frac{\rho}{\rho_w}\right) - p_b \tag{25}$$

and

$$\tau_{xz} = -\rho g z \left(\frac{\partial s}{\partial x} - \frac{1}{2}\frac{\partial h}{\partial x}\left(1 - \frac{\rho}{\rho_w}\right)\right) \tag{26}$$

where p_b is a buttressing term. A value of 250kPa was chosen for p_b, in order to reproduce ice shelf velocities similar to those observed at the outlet of the RIS. At the upstream boundary we apply the cryostatic pressure $\sigma_{xx} = \rho_i g(s-z)$. At the ice surface, a stress-free boundary condition of the form $\sigma_{ij} n_j = 0$ is used, where n_j is the outward unit vector normal to the surface.

The ocean pressure normal to the ice ocean interface (p_w) is applied as an elastic foundation, equivalent to a normal stress of:

$$p_w = -\rho_w g(z - w_a(t)) \tag{27}$$

where z is the depth below sea level and $w_a(t)$ is the time varying vertical tidal motion (Sect. 5.1).

Upstream of the grounding line, along the ice-bed interface (green and orange shaded regions in Figure 3), we use a Weertman style sliding law of the form

$$u = c\tau_b^m \tag{28}$$

where c is basal slipperiness, τ_b is the along-bed tangential component of the basal traction and m is a stress exponent. In all of our experiments we use a nonlinear sliding law with $m = 3$. Similarly, slipperiness values beneath the ice stream are kept fixed in all experiments to a value that approximately matches the mean flow velocity of the RIS. Beneath the margin, slipperiness is made several orders of magnitude smaller to restrict ice flow in this portion of the model.

We treat one side of the model ice stream as the medial line, since the problem is symmetrical ($\partial_y h = 0$), meaning we only need to model half of the ice stream with no lateral flow as the appropriate BC. The other side is treated as a grounded sidewall with no-slip, such that $u = v = w = 0$ (referred to hereafter as the clamped BC). In one of the experiments (**n3xy**) the constraint on vertical velocity is removed, as explained in Sect. 5.

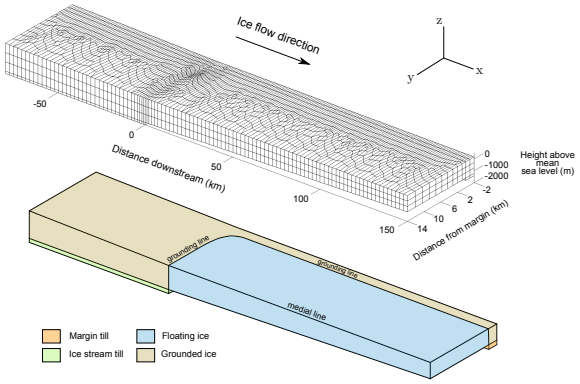

Figure 3. Finite element mesh used in the full-Stokes viscoelastic model (Sect. 4). Note that x and y horizontal scales have been reduced by factor 10 and 2 respectively.

4.3 Discretization

The model uses 20-node isoparametric hexahedral (brick) elements with a 27-point Gaussian integration scheme. These quadratic elements allow accurate representation of stresses and strains with much fewer numbers of elements than would ~~typically be used~~otherwise be needed when using linear elements. Element size varies from a maximum horizontal dimension of ∼2km to a minimum of ∼300m around the grounding line and in the shear margins. The finite element mesh is unstructured, with a GL that curves to avoid an unnatural grounding zone corner. The ice is 3 elements thick vertically, resulting in 9 integration points through its depth. The model mesh is shown in Fig. 3. The **n3xyz** simulation (Sect. 5) was repeated with double the horizontal resolution to check if this affected results. M_{sf} amplitude changed by a maximum of 3%, and ice velocity by a maximum of 2.5%, and so the default resolution was deemed sufficient.

5 Model Experiments

We conduct three simple model experiments to investigate the effects of flexural ice-softening within our model. Model runs are named such that **n1** or **n3** denotes whether we use a linear or nonlinear ice rheolgy and **xy** or **xyz** signifies which degrees of freedom are clamped on the sidewall boundary.

n3xyz In the first experiment we run the model with nonlinear ice rheology and sidewalls clamped in x, y and z. This is designed to simulate the 'Rutford' case whereby the margins are essentially stagnant and flexure occurs all along the GL, both where the main body of the ice stream meets the ocean and downstream of this point along the sides. In order to approximately match the observed 1m/d flow velocities of the floating portion of RIS we adjust the ice rate factor (A) uniformly.

n3xy For the second experiment we run the model as in **n3xyz** but the sidewalls downstream of the GL are not clamped vertically (z direction). With this setup there is no bending along the sidewalls downstream of the GL, so flexural stresses are only generated in the grounding zone around $x = 0$. This experiment is akin to a fast flowing ice-shelf bounded by stagnant floating ice, as can be found on the floating portion of some fast flowing outlet glaciers.

n1xyz The third experiment uses the same setup and boundary conditions as in **n3xyz** except that ice rheology is made linear, such that $n = 1$ in Eq. 22. This experiment is done to demonstrate the difference in response due only to changing n from one to three. In this experiment therefore, the ice viscosity is not stress-dependent, such that the bending stresses do not cause a reduction in the effective viscosity of ice. As such, it is not a 'realistic' situation (since ice is known to have a nonlinear rheology) but serves to emphasise that this nonlinearity is the important one at play in our model. In order to produce sensible ice-shelf velocities, the rate factor A is adjusted uniformly so that the background flow-speed (denoted u_{mean} in the previous analysis) is approximately the same as the other experiments.

5.1 Tidal Forcing

The time-varying vertical tidal forcing is implemented as a stress acting normal to the ice shelf base (Eq. 27). For all the experiments described above the model is forced with the principal semidiurnal (M_2 , S_2) and diurnal (O_1 , K_1) tidal constituents, i.e. the four tidal constituents which are generally largest beneath the Ronne Ice Shelf. Their amplitudes are derived from GPS measurements of vertical ice-shelf motion 20km downstream from RIS GL (**?**). The tidal forcing is kept intentionally simple to avoid complicating any interpretation of our full-Stokes model results.

6 Model Results

We now present results from our viscoelastic 3D full-Stokes model of an idealised ice-stream/shelf system. We begin by examining the modelled response at M_{sf} frequency, since previous models do not reproduce observations of this nonlinear effect on floating ice shelves. M_{sf} amplitude in horizontal surface ice displacements is shown in plan view for the three experiments in Fig. 4. For the **n3xyz** experiment, which can be thought of as the typical situation for a confined ice shelf subjected to large vertical tides, M_{sf} amplitude increases continuously downstream of the GL (Fig. 4a). In the across flow (y) direction the amplitude increases towards the medial line. Also shown are contours of ice-shelf velocity (u), which increase from 1 m/d upstream of the GL to more than 3 m/d on the shelf.

In the **n3xy** experiment the only change with respect to the **n3xyz** experiment is to remove the vertical clamp BC acting along the sidewall of the floating portion of the model. With this change in sidewall BC the M_{sf} amplitude is similar at the $x = 0$ GL where bending stresses are still generated.

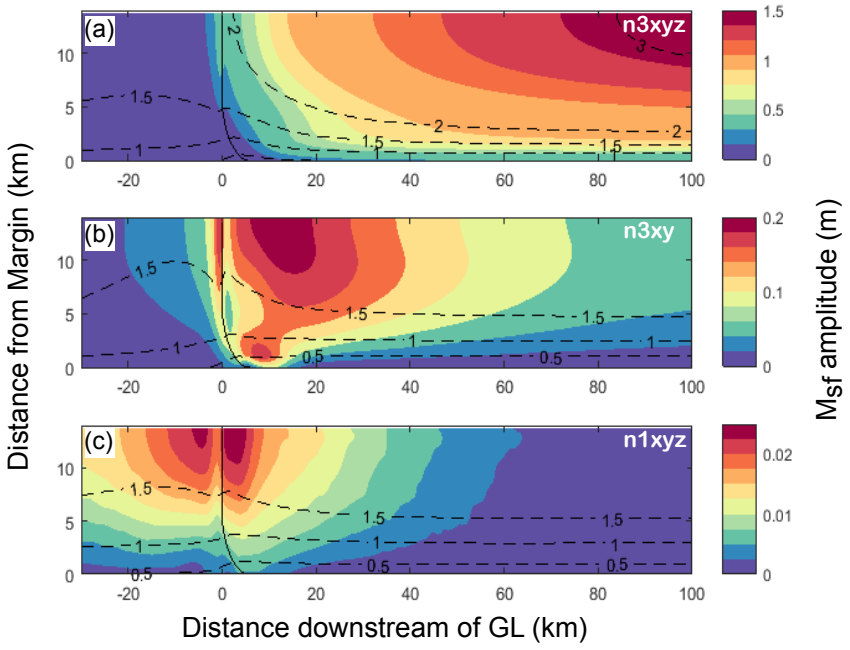

Figure 4. Plan view of M_{sf} amplitude in horizontal surface ice displacements, calculated with the full-Stokes viscoelastic model for the three experiments described in Secion 5. Panel a shows experiment **n3xyz**, i.e. the standard case with $n = 3$ and bending all along the sidewall boundary. Panel b shows experiment **n3xy** in which the ice only bends at the $x = 0$ GL. Panel c shows the **n1xyz** experiment, for which $n = 1$ but with the same BCs as panel a. Dashed black lines are contours of downstream mean surface ice velocity and solid black lines show the GL position. Note the differences in colour scale between each panel.

Downstream of this region however the M_{sf} amplitude decays rapidly ~~, reducing to almost zero far downstream~~ to zero with distance (Fig. 4b), ~~in contrast to~~ whereas in the **n3xyz** experiment ~~where the~~ the amplitude continues to increase with distance. Ice-velocities on the floating shelf are lower than in the **n3xyz** experiment, and ~~the 1 m/d contour is located further from the margin~~across-flow shear is less pronounced, such that the ice velocity contours are further apart.

For the **n1xyz** experiment, (Fig. 4c), where ~~ice rheology is linear but ice still bends all along the margins~~the only change compared to the **n3xyz** experiment is to change the value of n from one to three, the M_{sf} response is even more localised to the GL region and the amplitude is ~~far lower than the other two experiments.~~ close to zero.

Other tidal frequencies in the **n3xyz** experiment that emerge from the frequency doubling (Eq. 17), such as MS_4 , show very similar spatial patterns to the M_{sf} responses shown in Fig. 4a. In the **n1xyz** experiment, these frequencies are completely absent.

Running the standard **n3xyz** experiment with and without tides reveals how the mean ice-shelf flow is affected by tidal bending stresses. Averaging over the entire floating portion of the shelf, mean

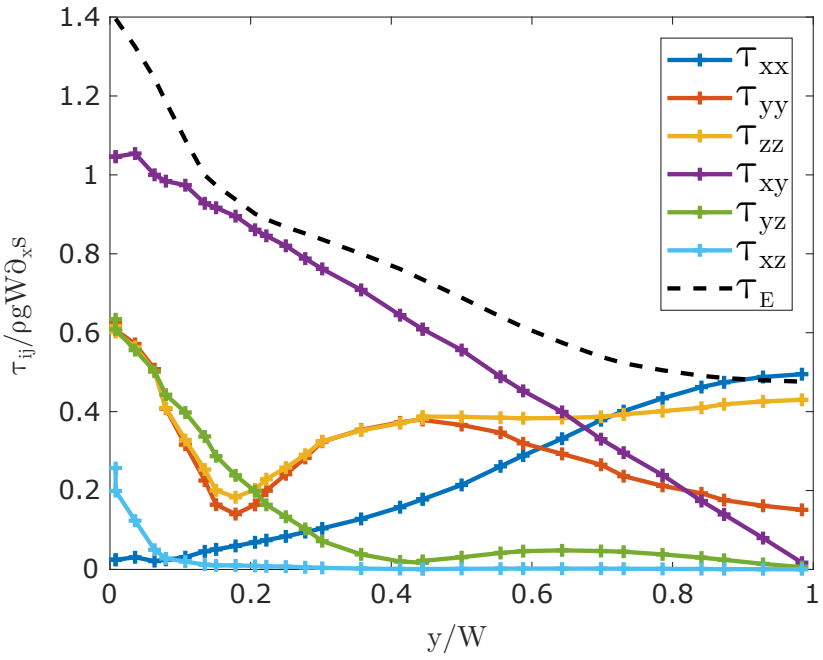

Figure 5. Across-flow transects of depth averaged non-dimensional stress from the full-Stokes viscoelastic model (Sect. 4) for experiment **n3xyz**. Profiles are taken 100 km downstream of the GL at high tide ($w_a = 2$ m). The stress scale is given by $\tau_{ij}/\rho g W \partial_x s$ and the length scale by y/W.

velocity is increased by ∼35% when the experiment is run with a vertical tidal forcing equivalent to that experienced near the RIS GL, as against with no tidal forcing.

~~Other tidal frequencies that emerge from the frequency doubling (17), such as , show very similar spatial patterns to the responses shown in Fig. 4, except that they are completely absent for the **n1xyz** experiment.~~

To explore the role of flexural stresses in more detail we plot across-flow profiles for each component of the deviatoric stress tensor (Fig. ~~??~~5). Stresses are taken from the **n3xyz** experiment at $x = 100$ km, to avoid the 2-D bending stresses at $x = 0$, and for a positive vertical tidal deflection of 2 m. The stress is ~~scaled~~ normalized by the depth-averaged horizontal shear stress at the margin $\rho g W \partial_x s$, as predicted by the analysis in Sect. 3 (for the ice-shelf surface slope in the model of 5.4×10^{-4} the stress scale is 67.5 kPa). Distance from the margin is ~~scaled~~ normalized by the ice-shelf half-width ($W = 14$ km).

Surface and bed across-flow bending stresses (τ_{yy}) are equal in amplitude but opposite in sign and so ~~we plot the depth average~~ all the stresses are plotted as the depth averages of their absolute values. This is more relevant for our purposes, since it is the absolute amplitudes of these stresses, and not their signs, that impact the effective stress. ~~For $w_a = 2$ m the~~

Our numerical results show that the contributions of across-flow ~~flexural stresses (τ_{yy}) reach ~ 40kPa and contributes a large portion of the total effective stress. Flexural stresses reduce to almost zero~~ and shear bending stresses to the effective stress, and therefore their relative impacts on effective ice viscosity, change significantly with increasing distance away from the ~~margin but then increase with opposite sign and once again contribute a large proportion of~~ ice-shelf margins. At the margins, both across-flow and shear bending stresses contribute about equally to the total effective stress~~up to a distance of ~ 12 km. Shear bending stresses (~~. With increasing distance away from the margins, both bending stress terms behave as damped cosine waves (Eqs. 4 and 5), however the resulting 'waveforms' are phase shifted with respect to one another. This can be seen in Fig. 5, where τ_{yy} shows a clear minimum at a distance of $y/W \approx 0.2$ before increasing again, whereas the minimum for τ_{yz} ~~) are of a similar size at the margin butdecay more rapidly towards the centerline~~is discernible at $y/W \approx 0.4$. As a consequence of this damped behaviour, bending stresses are largest near the grounding line but, for this geometry, have very little impact on effective viscosity along the ice shelf medial line where they have decayed to almost zero (the fact that τ_{yy} term is relatively large at the medial line is a result of ice-shelf spreading, not bending in the grounding zone). Note that, since λ is a function of ice thickness, the location of the bending stress minima will shift as the thickness changes.

At this stage we can briefly evaluate the validity of the assumptions made in Sect. 3. ~~A linear~~ The expression for the across-flow variation in τ_{xy} ~~matches very closely with the~~ , given by Eq. 3, varies from the value calculated by our full-Stokes model ~~results~~by a maximum of 5%. The assumption that $\tau_{yy} \approx -\tau_{zz}$ ~~is a good one~~ holds near the margin~~but breaks down towards the centerline where~~ , as shown in Fig. 5 where the modelled absolute values of these two stresses are approximately equal, but begins to break down at a distance of $W/2$ where the τ_{xx} becomes ~~important~~ increasingly large due to ice shelf spreading. Finally, the vertical shear stress (τ_{xz}) is ~~small everywhere , although shearing of grounded ice in the sidewalls does result in some stress on the neighbouring shelf~~approximately zero everywhere apart from within one ice thickness of the GL, where the effects of neighbouring ice shearing vertically in the grounded margin are felt. Nevertheless, even in this region τ_{xz} contributes less than 2% of the total effective stress.

Figure 6 shows the phasing of velocity, effective stress and strain heating rates in the model shear margin relative to vertical tidal motion (vertical motion is taken along the medial line to show the undamped tidal amplitude). Strain heating rate is calculated as $\dot{e}_E \tau_E / \rho C_p$, using a specific heat capacity of 1955.4 J/K (equivalent to an ice temperature of $-20°C$, **?**). This shows that modelled ice velocity, effective stress and strain heating are greatest just before high and low tide, as would be expected from a viscoelastic rheology. Effective stress in the shear margin is increased by over 50% during the highest tides of the spring cycle. Strain heating rate in the shear margin is enhanced by ~~the~~ vertical tidal motion ~~, which could partially~~ and so this mechanism could enhance the shear heating effect which has been invoked to explain the inferred softness of Ronne Ice Shelf shear margins (**?**).

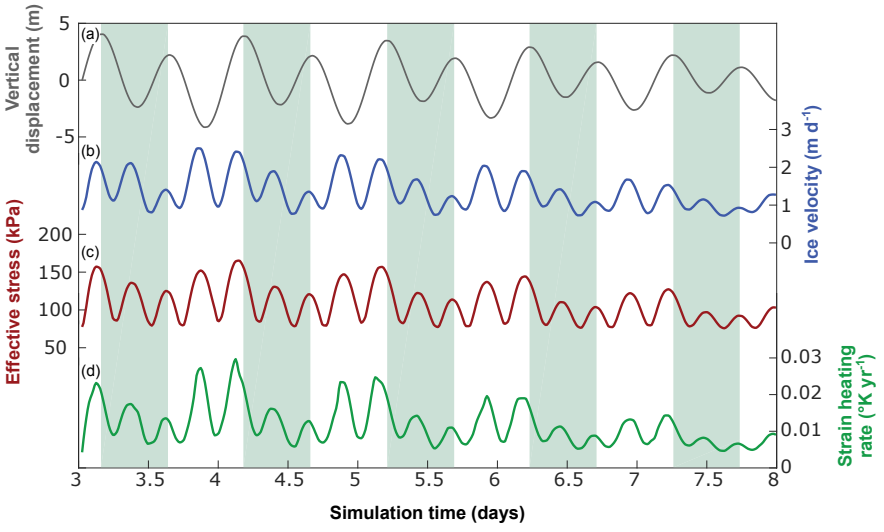

Figure 6. Time series of vertical ice displacement at the medial line (a), ice velocity (b), depth averaged effective stress in the shear margin (d) and depth averaged strain heating rate in the shear margin (e) from the 3D viscoelastic model. All variables are taken 100 km downstream from the main GL. The alternating blue and white shaded areas each represent one full tidal cycle, starting and ending at high tide.

7 Discussion

The analysis of Sect. 3, together with full-Stokes viscoelastic modelling, both suggest that flexural ice-softening could play an important role in the generation of the M_{sf} signal that is readily observed across the entire Ronne Ice Shelf (**?**). Flexural stresses due to vertical tidal motion can generate a fortnightly modulation in ice flow along any GL based only on the fact that ice is non-Newtonian. This mechanism is felt most strongly for a confined ice shelf, where bending occurs in the margins along the entire length of the shelf. New observations ~~of~~ reveal that the M_{sf} signal ~~reveal that it~~ is generally larger on ~~the floating ice shelf~~ ice shelves than on the adjoining ice streams, and tends to increase in amplitude in the downstream direction towards the ice front (**??**). Furthermore, the M_{sf} signal has now been observed to lead in phase on the ice shelf, casting some doubt on previous mechanisms that acted only on grounded ice (**?**). Our modelling work shows that flexural ice-softening can replicate this phasing and amplification of the M_{sf} signal downstream of ice stream GLs. Furthermore, these tidal bending stresses will lead to a net speed-up of the ice shelf.

Two alternative mechanisms have been proposed to explain the M_{sf} amplification on ice shelves, both reliant on GL migration. **?** argues that, if the sidewall GL migrates ~~a meaningful distance~~ over a tidal cycle, this will lead to a change in the effective width of the ice shelf as proportionally more of it ungrounds. Observed changes in the distance between the two maxima of lateral shear strain rate between high and low tide are interpreted as being caused by grounding line migration (**?**). An alternative explanation is that flexural ice-softening in the shear margins leads to a steepening of the

across-flow velocity profile at the boundary, thereby shifting the apparent margin as defined above. Calculating lateral shear strain rate 100 km downstream of the **n3xyz** simulation shows that each peak can shift by ∼500 m over a tidal cycle, leading to an apparent widening of 1 km even though there is no grounding line migration in the model. Alternative evidence of GL migration does exist in other parts of the FRIS (**?**) and this mechanism could be locally important, however, it seems unlikely that it could explain the pervasiveness of the M_{sf} signal across the entire shelf, since it is so reliant on local bedrock topography.

A previous modelling study has shown that GL migration is itself a strong nonlinearity which can generate an M_{sf} response in ice flow (**?**). **?** explored this idea in more detail and suggested that changes in the area which an ice shelf contacts the bed (due to GL and pinning point migration) is the dominant nonlinearity on RIS leading to the observed M_{sf} response. Within their framework, flexural stresses are ignored and the tidally varying ice shelf strain is a function of competing hydrostatic and buttressing stresses. ~~Due to the tunable nature of their approach, **?** were able to match many features of the observations however~~ The **?** model was flexible enough to allow for many of the observed aspects of the tidal modulation to be replicated. However, in the absence of a physically motivated model of GL migration, knowledge of the sub-shelf bathymetry, or even strong evidence for GL migration in the area, the extent to which this mechanism plays an important role remains an open one.

The flexural ice-softening mechanism produces a frequency doubling in the response of the ice shelf; since the marginal ice will be softest just preceding high and low tide. This is evident in the analysis of Sect. 3, which reveals that ice shelf velocity modulation will be dominantly at M_4 and MS_4 frequencies in contrast to the M_{sf} frequency which dominates the displacements. In order to check that our 3D viscoelastic model reproduces this behaviour we performed a tidal analysis on modelled displacement and velocity at the ice stream medial line, 100km downstream from the GL. Figure 7 shows the results of this tidal analysis as a frequency power spectrum, showing only constituents with a high signal to noise ratio. Surface horizontal displacements show a dominantly M_{sf} response, with almost no clear response at other frequencies (Fig. 7a). In the horizontal ice velocity (Fig. 7b) the M_4 and MS_4 frequencies emerge, with similar amplitudes to the M_{sf} in agreement to Eq. 17. Other nonlinear frequencies such as M_f, arising from interaction of the two diurnal tidal constituents, should be present but are not resolvable with a simulation time of sixty days.

As stated above, alternative mechanisms for generating an M_{sf} signal on floating ice assume that GL migration is the dominant process. Ice shelf velocities from the viscoelastic model proposed by **?** (using the parameters selected to match observations on RIS) are dominated by M_2 and S_2 frequencies. Since the mechanism is nonlinear, higher frequencies such as M_4 and MS_4 are also generated, but in that model are of a lower amplitude than the semidiurnal frequencies. In order to determine which mechanism is most likely responsible for observations on the RIS, therefore, we

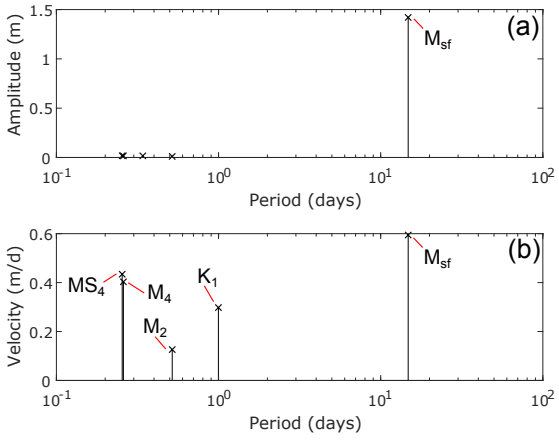

Figure 7. Tidal analysis of horizontal displacement (panel a) and velocity (panel b) from the full-Stokes model, taken at the medial line, 100km downstream of the GL. Notable tidal constituents are labelled with their respective names.

can look at whether short-term ice shelf velocity modulation is dominantly M_4 and MS_4 or M_2 and S_2 .

Most of our observations of the short-term velocity fluctuations on floating ice come from GPS units. Tidal analysis of these records is typically done on their measured displacements, rather than the much noisier velocities calculated from the time derivative of their measured position. By first fitting a tidal model to GPS measurements of horizontal ice flow downstream of the RIS, and then calculating the velocity from this smooth field, we can get a better velocity signal with which to do further analysis. A convenient measure of the importance of each tidal constituent is the percent energy (PE) (**?**). Tidal analysis with Utide (**?**) of the measured horizontal ice displacements 20 km downstream of RIS GL show that the M_{sf} signal dominates with 87% of PE, followed by the diurnal and semidiurnal tidal constituents. Analysis of the velocites, calculated as described above, reveals that the two largest constituents are MS_4 and M_4 with 21% and 11% of PE, respectively. Based on the arguments given above, these results provide compelling evidence that the flexural ice-softening mechanism is responsible for the majority of the observed M_{sf} signal on the RIS.

One consequence of not including GL migration in our model is to generate artificially large stresses at the GL during high tide, where ~~flexural~~ tidal stresses are acting to lift the ice from the bed but the clamped boundary condition prevents this from happening. For comparison, stresses were obtained for a simulation in which the GL was allowed to migrate, forced by a positive two metre tidal deflection. At the GL node, effective stress was 67% greater in the pinned case, but this effect is highly localised and depth averaged effective stress at the GL is only 12% greater. If bed geometry on RIS is such that the GL can migrate a meaningful distance, our model would slightly overestimate the reduction in shear margin effective viscosity due to bending stresses at high tide. Our aim here is

to investigate the flexural ice-softening mechanism in isolation and including GL migration would complicate any interpretation, particularly given the unknown bed geometry of RIS. GL migration could play a role in generating the M_{sf} signal observed across the Ronne Ice Shelf, depending on whether the local bed geometry permits it. That being said, both the simplicity of the flexural ice-softening mechanism, together with the ease with which it explains many aspects of the observed tidal modulation in ice-shelf flow, suggest that it is likely to be the primary mechanism at play.

In all our full-Stokes model experiments the M_{sf} signal decays rapidly upstream of the grounding line, contrary to observations which show the signal persists at least ~80 km upstream of the Rutford, Evans and Foundation Ice Stream GLs (**???**). Previous studies have proposed that a nonlinear basal sliding law could generate the M_{sf} signal on grounded ice (**????**). ~~This model~~ The model presented in this paper also uses a nonlinear sliding law~~but~~ , but when the flexural softening mechanism is absent and the nonlinear sliding law is the only mechanism at play (experiment **n1xyz**) it fails to reproduce the observed M_{sf} amplitude and decay length scale ~~when that is the only mechanism at play (experiment **n1xyz**.~~(Fig. 4c). Other mechanisms have been suggested which could promote propagation of this signal far upstream, for example weakened margins or tidal pressurisation of the subglacial drainage system (**??**). Since our focus is on the ice-shelf we do not include any of these mechanisms in this model.

The flexural softening mechanism which we have described acts in the grounding zone which may often coincide with a shear margin, a portion of the ice sheet that is complex and remains poorly understood. Shear margins are typically heavily crevassed due to the intense shear straining, making them difficult to access and instrument. These crevasses change the effective bulk properties of the ice, altering the flexural profile compared with undamaged ice (**?**). Furthermore, repeated straining will alter the ice fabric and make it highly anisotropic (**??**). In the grounding zone, repeated tidal straining may itself alter the ice fabric, although this has never been investigated to our knowledge. Finally, lateral and tidal straining will cause strain heating (Fig. 6d). A consequence is that ice within floating shear margins subjected to large tides may be warmer as a result of tidal flexure, although the presence of crevasses ~~would~~ could lead to a complex depth-dependent temperature profile (**??**). All of the processes described above will interact with tidal flexure and further modelling is required to evaluate their effects in detail.

Remote sensing techniques suggest that the amplitude of the M_{sf} signal shows considerable spatial heterogeneity (**?**). There remains some debate about the correct value for the ice rheological exponent n and whether it might vary spatially (**?**, and references therein), although this is often conveniently ignored in modelling studies. Since the amplitude of the M_{sf} signal on the ice shelf is highly sensitive to the value of n, further modelling of this effect might help to provide new insights into ice rheology. For example, it might be that the observed spatial pattern and magnitude of the M_{sf} effect on the shelf downstream of RIS can only be reproduced for certain choices of n, although it would be difficult to separate this from other factors at play. In the context of the flexural-ice softening mechanism, this

heterogeneity could also arise due to variation in ice properties such as thickness, fabric, damage, etc.

8 Conclusions

We present results from both analytical and full-Stokes models, which show that tidal bending stresses in ice-shelf margins can give rise to large scale temporal variations in ice flow. The non-linear rheology of ice means that, as an ice-shelf bends to accomodate vertical tidal motion, stresses generated in the grounding zone reduce the effective viscosity of ice. This leads to modulation of ice-shelf velocity at a number of frequencies, including the M_{sf} frequency which is readily observed on many Antarctic ice shelves (**????**). In addition, the nonlinear response changes the mean flow of the ice shelf when it is subjected to vertical tidal motion.

This mechanism relies only on the nonlinear rheology of ice and can explain many recent GPS and satellite observations of tidal effects on ice-shelf flow. ~~Unlike previous mechanisms~~By causing an increase in ice velocity twice during one tidal cycle, it leads to a strong frequency doubling effect which is potentially diagnosable from careful measurement of ice-shelf velocity with high ~~temporaly~~ temporal resolution and accuracy. Tentative analysis of GPS measurements from the floating portion of RIS suggest that these characteristic frequencies can be seen in existing data and that their relative amplitudes match those of our model.

The bending stresses investigated in this study are typically ignored and difficult to incorporate into large-scale ice-sheet models, however this work shows that these stresses have a role to play in the overall flow-regime. Full-Stokes modelling of a tidally energetic region such as the FRIS would lead to further insights into the importance of this mechanism, its relevance for ice flow models and possibly even ice rheology.

Appendix A: Derivation of across-flow shear stress

We start from the simplified z-momentum given in Eq. 2b, together with expressions for the bending stresses τ_{yy} and τ_{yz} (Eqs. 4 and 5 respectively). Applying the surface boundary condition $\sigma\hat{\mathbf{n}} = 0$ we find that

$$-\partial_y s\,\tau_{yz}(s) + \sigma_{zz}(s) = 0. \tag{A1}$$

Since $\tau_{yz} = 0$ at the surface, this reveals that $\sigma_{zz}(s) = 0$.

Using this result and integrating the z-momentum (Eq. 2b) from the surface to arbitrary depth z we arrive at an expression for $p(x, y, z, t)$:

$$p = \rho g(s - z) - \tau_{yy}(z) - \int_z^s \partial_y \tau_{yz}\, dz. \tag{A2}$$

Inserting this into the x-momentum of Eq. 2a gives

$$\partial_y \tau_{xy} = \rho g \partial_x s - \partial_x \tau_{yy} - \partial_x \int_z^s \partial_y \tau_{yz}\, dz, \tag{A3}$$

where

$$\partial_x \tau_{yy} = \frac{9 w_a z h^{-5/2} \partial_x h \sqrt{\rho_w E g}}{\sqrt{3(1-\mu^2)}} e^{-\lambda y} \Big[\sin(\lambda y) + (\lambda y - 1)\cos(\lambda y) \Big], \tag{A4}$$

$$\partial_x \int_z^{\hbar} \partial_y \tau_{yz}\, dz = -\frac{3}{4} \rho_w g w_a \partial_x h (h - 2z) h^{-4} e^{-\lambda y} \Big(2\zeta \big[\sin(\lambda y) + \cos(\lambda y) \big] + \lambda y \big[h^2 - \zeta \big] \sin(\lambda y) \Big) \tag{A5}$$

and $\zeta = z(h + 2z)$. Note that the x dependence of Eq. A2 is through the ice thickness h, which also appears in the expression for λ (Eq. 6). Integrating from the surface to the bed and dividing by ice thickness yields the depth averaged across-flow gradient in horizontal shear stress:

$$\partial_y \overline{\tau_{xy}} = \rho g \partial_x s - \frac{1}{h} \int_b^s \partial_x \int_z^s \partial_y \tau_{xy} dz. \tag{A6}$$

With the boundary condition that $\overline{\tau_{xy}}$ is zero at the centerline, we can integrate along y to give an expression for depth averaged horizontal shear stress, which is

$$\overline{\tau_{xy}} = \rho g h \partial_x s - \frac{3 \rho_w g w_a \partial_x h e^{-\lambda y} \lambda y \sin(\lambda y)}{4h}. \tag{A7}$$

It turns out that the second term on the R.H.S. of Eq. A7 is much smaller than the other two for any sensible choice in parameters and so the horizontal shear stress is balanced by the driving stress term to a very good approximation. Since the geometry along the x direction does not change with time the only temporal variation in τ_{xy} enters through the smaller second term. As such, $\dot{\tau}_{xy} \approx 0$; a curious finding given the large changes in centerline velocity but one that is borne out by examination of the stresses in our full-Stokes model (Sect. 6).

For a comparison with the idealised system of equations presented above, we take a 2-D slice through the ice shelf in the full-Stokes model (presented in Sect. 4) and look at the deviatoric stresses. We take this slice far away from the GL at $x = 0$ to avoid the additional bending stresses in this region. The lateral shear stress τ_{xy} is found to vary linearly from zero at the medial line to ~70kPa at the margin and is approximately constant with depth (see also Fig ??5). Maximum variation in τ_{xy} over a tidal cycle is ~3%, despite the ice velocity doubling at the medial line. This matches closely with the profile predicted by Eq A7 using parameters taken from the model. The main discrepancy in stresses between the full-Stokes model and the simplified system of Eq. 2a is that modelled τ_{xx} becomes relatively large near the medial line, however since this is not the case near the margins, where most of the lateral shearing takes place, the approximation appears to not be a bad one.

Appendix B: Analytical solution for double clamped elastic beam

Much of the work on tidal bending of floating ice is based on beam theory, specifically the analysis of elastic beams on elastic foundations first explored by **?**. The classical solution for bending of a floating ice tongue was first derived by **?** and has since been used extensively in studies of ice flexural process (**?????????**). We will call this set of equations the long beam model (LBM). The set of boundary conditions (BCs) chosen in the LBM are as follows:

$$\left.\begin{aligned} w &= 0 \\ w' &= 0 \end{aligned}\right\} y = 0 \qquad \left.\begin{aligned} w &= w_a \\ w' &= 0 \end{aligned}\right\} y \to \infty \tag{B1}$$

where $w(y)$ is the vertical deflection of the neutral axis and w_a is the change in sea level due to tides. The assumption in Eq. B1 that ice is freely floating at the far-field boundary is valid in many circumstances, however the shelf downstream of RIS is only $\sim 30\,\mathrm{km}$ wide and so this set of BCs might not be appropriate. A better set of BCs for a narrow ice shelf consists of a beam clamped at both ends, such that

$$\left.\begin{aligned} w &= 0 \\ w' &= 0 \end{aligned}\right\} y = 0 \qquad \left.\begin{aligned} w &= 0 \\ w' &= 0 \end{aligned}\right\} y = 2W \tag{B2}$$

Starting from the beam equation for a floating ice shelf:

$$w^{IV}(y) = -\frac{12(1-\nu^2)}{Eh^3}\rho_w g(w_a(t) - w(y)), \tag{B3}$$

subject to the BCs in Eq. B2, we arrive at the solution:

$$w(y,t) = w_a(t)\left[1 - e^{-\lambda y}\left(C_1\sin(\lambda y) + C_2\cos(\lambda y)\right) + e^{\lambda y}\left(C_3\sin(\lambda y) + C_4\cos(\lambda y)\right)\right], \tag{B4}$$

where λ is given in Eq. 6 and the constants C_1 to C_4 are:

$$C_4 = \frac{1 - e^{2\lambda W}(\cos(2\lambda W) + \sin(2\lambda W))}{e^{4\lambda W} + 2e^{2\lambda W}\sin(2\lambda W) - 1} \tag{B5a}$$

$$C_2 = 1 + C_4 \tag{B5b}$$

$$C_3 = \frac{e^{2\lambda W}(\cos(2\lambda W) - \sin(2\lambda W)) - 1}{e^{4\lambda W} + 2e^{2\lambda W}\sin(2\lambda W) - 1} \tag{B5c}$$

$$C_1 = 1 + \frac{2\tan(2\lambda W)}{e^{4\lambda W}\tan(2\lambda W) + \tan(2\lambda W) + e^{4\lambda W} - 1} + C_4\left(\frac{e^{4\lambda W} + (3e^{4\lambda W} - 1)\tan(2\lambda W) - 1}{e^{4\lambda W} + (1 + e^{4\lambda W})\tan(2\lambda W) - 1}\right). \tag{B5d}$$

If the product λW is large (specifically, large in comparison to π) then the hinge zone is narrow compared to the ice shelf width. In this situation, $C_1 \approx C_2 \approx 1$ and $C_3 \approx C_4 \approx 0$, such that Eq. B4

reduces to the LBM solution (**?**). As it turns out, for the RIS where $W \approx 14$ km, this turns out to be the case and so the simpler LBM differs only very slightly from the solution given in Eq. B4. As a result, we can safely use the LBM to approximate bending stresses on the RIS.

590 *Acknowledgements.* We are grateful to Rob Arthern, Brent Minchew and Teresa Kyrke-Smith for very helpful discussions. S. Rosier was funded by the UK Natural Environment Research Council large grant "Ice shelves in a warming world: Filchner Ice Shelf System" (NE/L013770/1).

References